J|A|C|S
ARTICLES
Published on Web 03/07/2007

Single-Crystal Nanoribbons, Nanotubes, and Nanowires from Intramolecular Charge-Transfer Organic Molecules

Xiujuan Zhang,[†] Xiaohong Zhang,*[,†] Kai Zou,[†] Chun-Sing Lee,[‡] and Shuit-Tong Lee*[,†,‡]

Contribution from the Nano-organic Photoelectronic Laboratory and Laboratory of Organic Optoelectronic Functional Materials and Molecular Engineering, Technical Institute of Physics and Chemistry, Chinese Academy of Sciences, Beijing 100101, China, and Center of Super-Diamond and Advanced Films (COSDAF) & Department of Physics and Materials Science, City University of Hong Kong, Hong Kong SAR, China

Received June 15, 2006; E-mail: xhzhang@mail.ipc.ac.cn; apannale@cityu.edu.hk

Abstract: Single-crystal one-dimensional (1-D) nanostructures of [2-(*p*-dimethyl-aminophenyl)ethenyl]-phenyl-methylene-propanedinitrile (DAPMP) have been prepared by a simple solution process without the assistance of added surfactant, catalyst, or template under ambient condition. The approach exploits the directional supramolecular interaction induced by strong donor−acceptor dipole−dipole supramolecular interaction in the growth of 1-D nanostructures. By varying the process temperatures, the DAPMP nanostructures can be controllably prepared as either nanoribbons, nanotubes, or nanowires with high morphological and chemical purities. Significant changes in optical properties were observed for nanostructures of different morphology.

Introduction

The ability to prepare nanostructures with defined morphologies and sizes in bulk scale is an essential requirement for applications of nanomaterials. As a result, extensive efforts have been devoted to developing synthetic capabilities to produce nanomaterials with tailored electronic and photonic properties. To date, much attention has focused on preparing inorganic nanostructures with controlled morphologies.[1−6] Nanostructures of organic small-molecule materials are also of interest, due to the tunable electronic and optical properties as well as greater variety and flexibility of these materials via molecular design.[7,8] In addition, morphology also plays an influential role in determining the properties of organic nanostructures. By comparison, progress has been slow in the synthesis of organic nanostructures, and our ability to control the morphology and size of organic nanomaterials lags far behind their inorganic counterparts. There is, therefore, an intense interest in improving the preparation methods to control the morphology and size of organic nanostructures.

In this work, we report a simple solution method, which can controllably prepare [2-(*p*-dimethyl-aminophenyl)ethenyl]-phenyl-methylene-propanedinitrile (DAPMP) in the form of single-crystal nanoribbons, nanotubes, and nanowires in large quantities and with high morphological and chemical purity. DAPMP is a typical intramolecular charge-transfer (ICT) compound and is regarded as an ideal candidate for nonlinear optical material because it possesses high up-conversion fluorescence efficiency.[9] ICT molecules are characterized by an electron-donating (D) and an electron-accepting (A) group connected through π-conjugation. We have recently found that the direction of D−A dipole−dipole attraction between ICT molecules can be used to guide the preferential growth of 1-D or semi-1-D nanomaterials.[10] In this paper, we report that, by changing the processing temperature, single-crystal nanostructures of DAPMP with different morphologies could be controllably obtained. Significantly, changes in morphology are accompanied by changes in optical properties of these nanomaterials. Our results thus suggest a viable approach for making single-crystal nanostructures with custom-tuned morphologies and properties.

[†] Chinese Academy of Sciences.
[‡] City University of Hong Kong.

(1) Zhang, J.; Sun, L. D.; Yin, J. L.; Su, H. L.; Liao, C. S.; Yan, C. H. *Chem. Mater.* **2002**, *14*, 4172−4177.
(2) Dick, K. A.; Deppert, K.; Larsson, M. W.; Martensson, T.; Seifert, W.; Wallenberg, L. R. *Nat. Mater.* **2004**, *4*, 380−384.
(3) Trewyn, B. G.; Whitman, C. M.; Lin, V. S. *Nano Lett.* **2004**, *4*, 2139−2143.
(4) Kang, Z. H.; Wang, E.; Mao, B. D.; Su, Z. M.; Gao, L.; Lian, S. Y.; Xu, L. *J. Am. Chem. Soc.* **2005**, *127*, 6534−6535.
(5) Wen, X. G.; Wang, S. H.; Ding, Y.; Wang, Z. L.; Yang, S. H. *J. Phys. Chem. B.* **2005**, *109*, 215−220.
(6) Zhao, Y. P.; Ye, D. X.; Wang, G. C.; Lu, T. M. *Nano Lett.* **2002**, *2*, 351−354.
(7) (a) Kasai, H.; Kamatani, H.; Okada, S.; Oikawa, H.; Matsuda, H.; Nakanishi, H. *Jpn. J. Appl. Phys.* **1996**, *35*, L221−L223. (b) Zhang, X. J.; Ju, W. G.; Gu, M. M.; Zhang, X. H.; Meng, X. M.; Shi, W. S.; Lee, C. S.; Lee, S. T. *Chem. Commun.* **2005**, *33*, 4202−4204. (c) Zhang, X. J.; Zhang, X. H.; Meng, X. M.; Shi, W. S.; Lee, C. S.; Lee, S. T. *J. Phys. Chem. B* **2005**, *109*, 18777−18780.
(8) (a) Heo, J. S.; Park, N. H.; Ryu, J. H.; Suh, K. D. *Adv. Mater.* **2005**, *17*, 822−826. (b) Hu, D. H.; Yu, J.; Padmanadan, G.; Ramakrishanan, S.; Barbara, P. F. *Nano Lett.* **2002**, *2*, 1121−1124. (c) Nguyen, T. Q.; Bushey, M. L.; Brus, L. E.; Nuckolls, C. *J. Am. Chem. Soc.* **2002**, *124*, 15051−15054. (d) Fu, H. B.; Xiao, D. B.; Yao, J. N.; Yang, G. Q. *Angew. Chem., Int. Ed.* **2003**, *42*, 2883−2886. (e) Chiu, J. J.; Kei, C. C.; Perng, T. P.; Wang, W. S. *Adv. Mater.* **2003**, *15*, 1361−1364.
(9) Wang, H. Z.; Zheng, X. G.; Mao, W. D.; Yu, Z. X.; Gao, Z. L.; Yang, G. Q.; Wang, P. F.; Wu, S. K. *Appl. Phys. Lett.* **1995**, *66*, 2777−2779.
(10) Zhang, X. J.; Zhang, X. H.; Chang, J.; Lee, C. S.; Lee, S. T., in preparation.

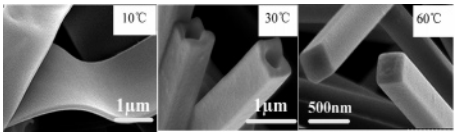

Figure 1. Typical SEM images of nanostructures with different morphologies.

Experimental Section

Materials. All compounds used here were synthesized in-house, and molecular structures were confirmed with nuclear magnetic resonance (NMR) and mass spectroscopy (MS). High-purity water (resistivity = 18.2 MΩ cm) was generated with a Milli-Q apparatus (Millipore) and was filtered using an inorganic membrane with a pore size of 0.02 μm (Whatman International, Ltd.) just before use. Tetrahydrofuran (THF) was obtained from Beijing Chemical Agent, Inc., and was used as received without further purification.

Preparation. Organic nanostructures were prepared by a simple solution process. DAPMP was dissolved in THF to a concentration of 2×10^{-3} M. 200 μL of this solution was injected into 5 mL of high-purity water with stirring, and the water was maintained at different temperatures from 0 to 60 °C. After being stirred for 3 min, the sample was left undisturbed for about 4 h to stabilize the nanostructures.

Characterization. The sizes and shapes of the nanostructures were observed with a field-emission scanning electron microscope (FESEM, Hitachi S-4300) operated at an accelerating voltage of 5 kV. For SEM studies, a few drops of the sample were placed onto silicon substrates, and the solvent was left to evaporate. To minimize sample charging, the dried samples were coated with a thin gold layer (<5 nm) right before SEM examination. Samples for transmission electron microscopy (TEM) were prepared by placing a drop of the suspended sample on a holey copper TEM grid (i.e., coated with carbon film) and then dried in air for a few hours before observation. The TEM study was performed in a Philips CM200FEG microscope operating at an accelerating voltage of 200 kV. Fluorescence spectra were measured with an excitation wavelength at 480 nm using a Hitachi F-4500 spectrometer. The X-ray diffraction (XRD) patterns were recorded with a Japan Mac Science M18AHF X-ray diffractometer equipped with Cu Kα radiation (λ = 1.54050 Å), employing a scanning rate of 4 deg/min in the 2θ range from 3° to 50°.

Computational Method. The configurations of ICT compounds were optimized from the corresponding minimum energy process using the B3LYP/6-31G* method in Gaussian 98.

Results and Discussion

Figure 1 shows the typical SEM images of nanostructures with different morphologies. Details of the nanostructures prepared at different temperatures are illustrated in Figure 2. When the experiment was carried out at 0 °C, ribbon-like structures with smooth surfaces were obtained (Figure 2a). These ribbons have a width of about 180 nm, a thickness of 30−40 nm, and a length of up to 20 μm. The SEM images show that the nanoribbons have high morphological purity, and nanostructures of other morphologies are seldom observed in the samples. It should be pointed out that no surfactant, template, or catalysis is needed in the present process. In fact, other than the source organic materials, only two solvents (water and a relatively small amount of THF) are used in the process, therefore yielding high-purity nanomaterials free from contaminations. As DAPMP is virtually insoluble in water, practically all DAPMP molecules are segregated and assembled to form the nanoribbons in the water. To confirm the composition and purity of the as-prepared nanostructures, the samples were redissolved in dichloromethane (CH_2Cl_2), and the absorption and emission spectra of the solutions were measured. The spectra are identical to those of the original dilute CH_2Cl_2 solutions of DAPMP. Furthermore, NMR and MS measurements also confirmed that the microstructures only consist of original molecules with no detectable impurities.

When the process temperature was increased to 10 °C, the dimensions of the nanoribbon obtained (Figure 2b) are substantially increased. The resulting nanoribbons have an average width of 2 μm and a thickness of 70−80 nm. Similar to the nanoribbons prepared at 0 °C, the large ribbons also have smooth surfaces, high morphological, and chemical purity, and they were prepared with almost quantitative yield. Typical width-to-thickness ratios of the nanoribbons increase from 4.5 to 25 as the temperature increases. As the temperature of preparation was increased to 18 °C, nanotubes (Figure 2c) were obtained instead of nanoribbons. The nanotubes have a width of about 1 μm and a length of 15−25 μm, with smooth and flat surfaces and sharp open ends. Occasionally, two to three of these tubes are fused together at a single junction (marked by white circles in Figure 2c). When the temperature was further increased to 30 °C, the outer width of the nanotubes decreased (Figure 2d). At 40 °C, some of the nanotubes grew into solid nanowires (Figure 2e). Fusion of several tubes at a single junction could be observed occasionally (not shown here), but fusion occurred much less frequently than at 18 °C. The growth trend continued as temperature increased to 60 °C, when all of the products became solid nanowires as shown in Figure 2f. The wires are about 250 nm in width and 20 μm in length with rectangular cross-sections.

The nanostructures were further examined with TEM, the results of which basically confirm the morphology as observed by SEM. Figure 3a shows the typical TEM images of the nanoribbons prepared at 10 °C, while Figure 3b and c shows the TEM images of the nanotubes formed at 30 °C and the nanowires at 60 °C, respectively. All of the insets in Figure 3 depict the corresponding selected area diffraction (SAD) patterns of the nanostructures. The sharp diffraction spots in these SAD images indicate that all of the nanostructures are single crystalline. The structures of the nanoribbons, nanotubes, and nanowires were investigated by XRD analysis (Figure 4).[11] The sharp peaks in the XRD patterns also confirm the nanostructures are highly crystalline. More importantly, the XRD patterns of nanotubes and nanowires are essentially the same and similar to that of starting powder materials, but are obviously different from that of nanoribbons. Analysis showed that the crystal structure of nanotubes and nanowires is tetragonal, while that of nanoribbons is monoclinic (see Supporting Information, Part S1). We therefore conclude that nanoribbons and nanotubes/nanowires are different polymorphic structures of DAPMP. It is significant that these polymorphic structures can be obtained in high purity in a relatively narrow temperature range from 0 to 60 °C.

The above results show that the morphologies of DAPMP nanostructures can be easily controlled by varying the processing temperature. Effects of other processing parameters, including initial concentration of the solution, stirring time, aging time, and rate of addition of DAPMP/THF solutions to water, have

(11) Dong, C. *J. Appl. Crystallogr.* **1999**, *32*, 838−838.

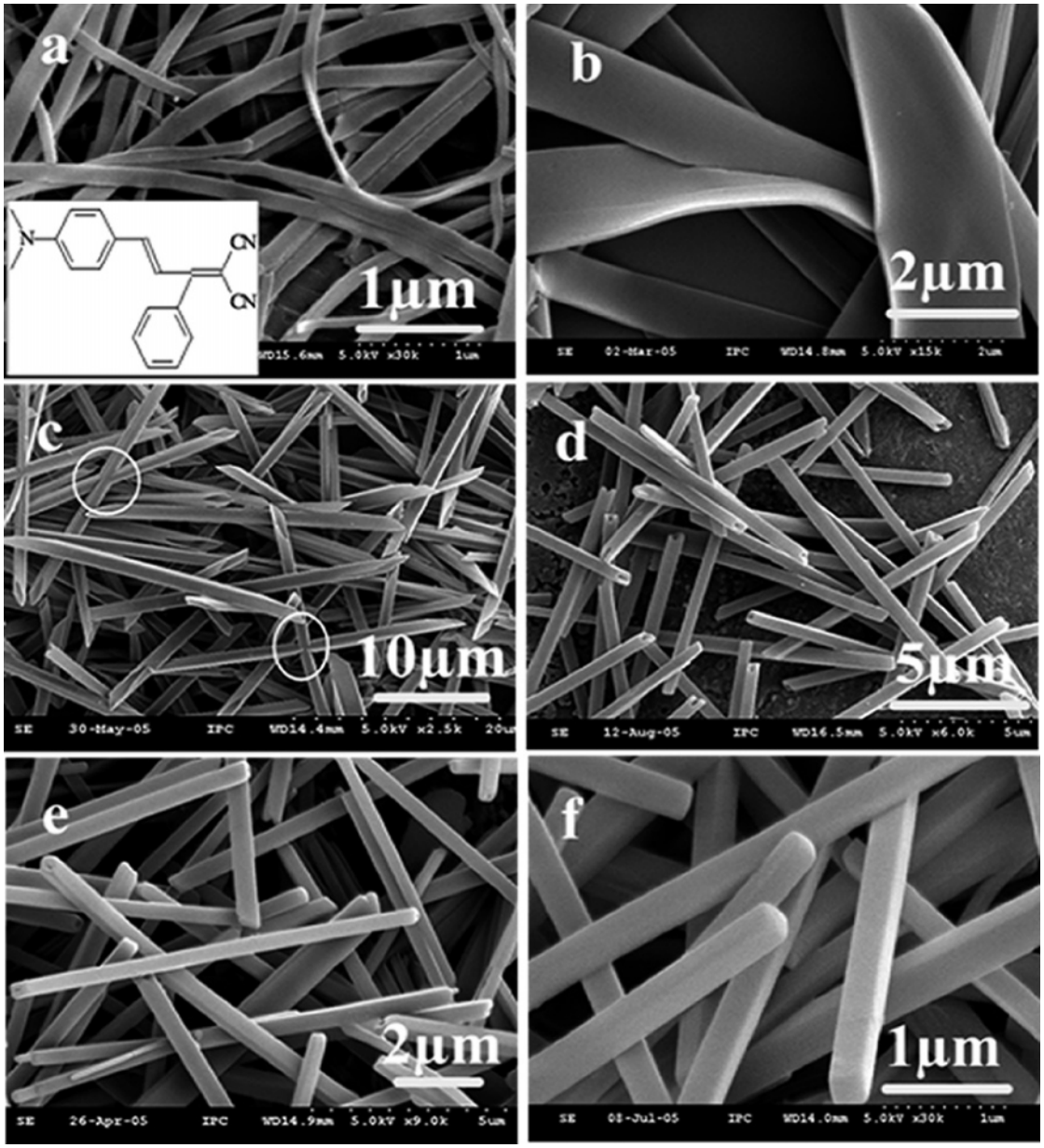

Figure 2. SEM images of DAPMP nanostructures prepared at different temperatures: (a) 0 °C, (b) 10 °C, (c) 18 °C, (d) 30 °C, (e) 40 °C, and (f) 60 °C. Inset in (a) shows the molecular structure of DAPMP.

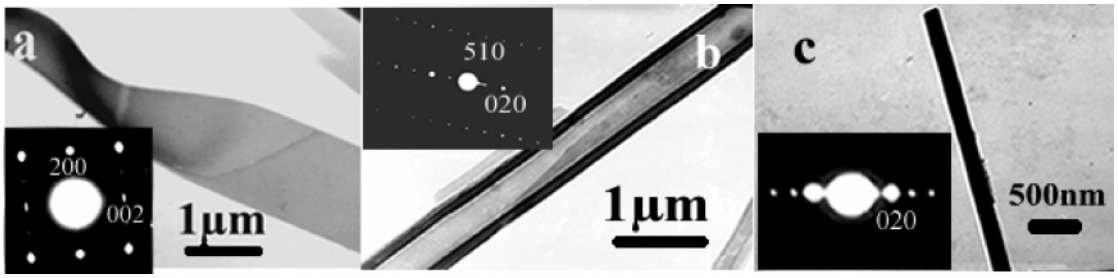

Figure 3. TEM images of DAPMP nanostructures: (a) nanoribbon prepared at 10 °C, (b) nanotubes prepared at 30 °C, and (c) nanowires prepared at 60 °C. Insets in each image show the corresponding SAD pattern.

also been investigated. These parameters resulted only in minor changes in the dimensions and the shape of nanostructures. Further, when *N*,*N*-dimenthylformamide (DMF) or dimethylsulfoxide (DMSO) was used instead of THF to dissolve DAPMP, the changes of morphology were not as obvious as that of THF upon varying the process temperature.

The temperature-induced morphological change from semi-1-D nanoribbon to 1-D nanotube and solid nanowire is remarkable, although the mechanism of the changes is not at all clear. On the basis of the experimental results together with those from a series of other similar molecules (listed in Figure 5), we suggest that the change of semi-1-D nanoribbons to 1-D

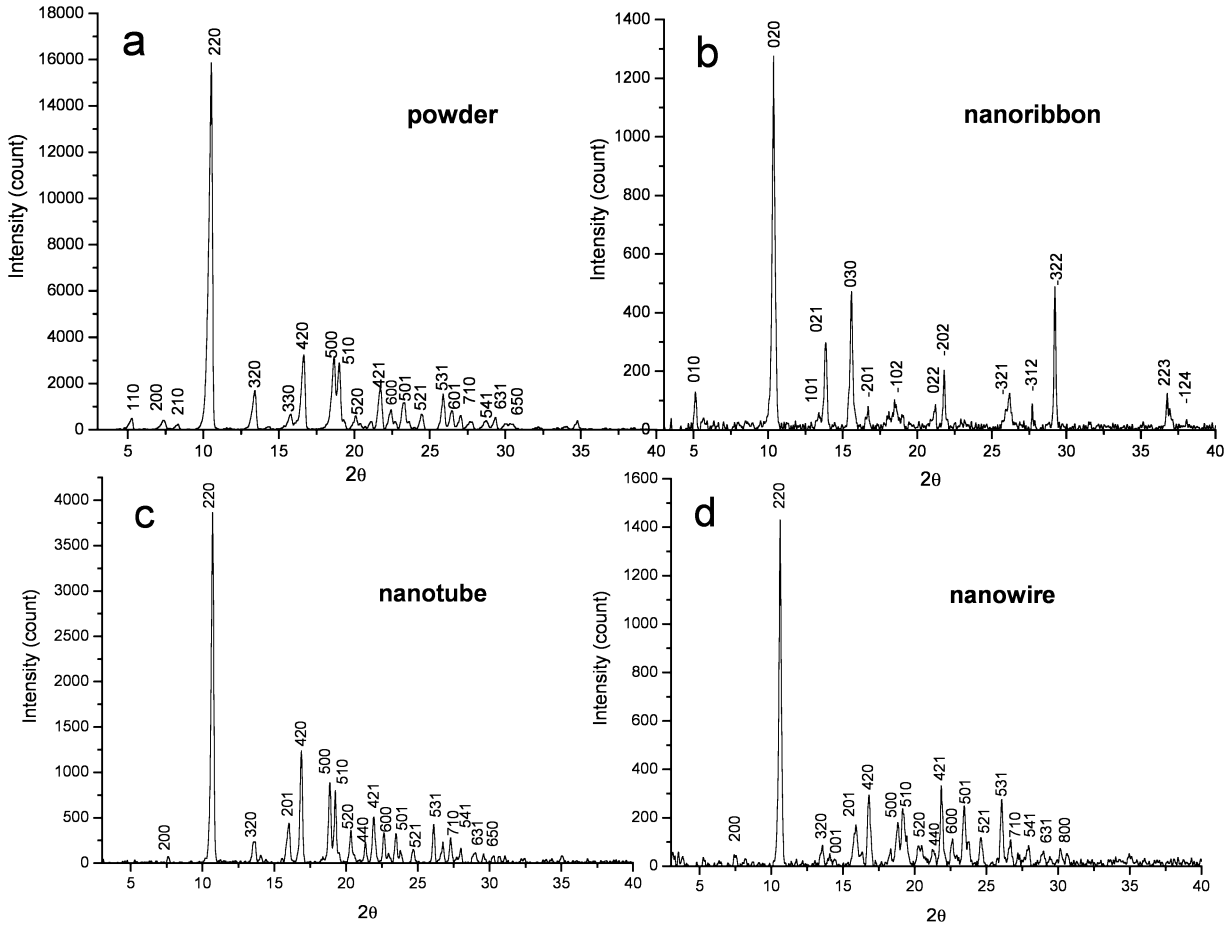

Figure 4. XRD patterns of DAPMP bulk powder materials (a), nanoribbons (b), nanotubes (c), and nanowires (d).

nanotubes is attributable to the different pathways of low-energy molecular stacking at different temperatures, which are elucidated as follows.

To better understand the formation process of DAPMP nanostructures, the morphology evolution of DAPMP is compared to the nanostructures prepared from [4-(dimethylamino)-phenyl]methylene **(**DPM), which also has the characteristics of a strong donor−acceptor structure. The SEM images (Figure 5a) of the nanostructures prepared from DPM reveal that only 1-D nanowires could be obtained under all processing conditions. The striking difference in the nanostructures arising from DAPMP and DPM may be attributed to the difference in molecular configurations as shown in Scheme 1, which were obtained from optimization using the B3LYP/6-31G* method in Gaussian 98.

For DPM, both the donor and the acceptor groups are completely aligned in one direction (D−A type), and the organic molecules would aggregate along this direction. In the case of DAPMP, besides the strong electron-releasing moiety of the *N*,*N*-dimethyl group, the weaker electron-releasing phenyl moiety lies in the direction about 90° perpendicular to the long molecular axis, as shown in Scheme 1a. As a result, DAPMP can be regarded as having two dipole−dipole interactions (D−A−D type) in two different directions, which could induce molecular aggregations along the two directions. We propose that the direction(s) of the dipole moments would dictate the favored direction(s) of molecular stacking and thus the resulting morphologies. Two distinct directions of interaction (D−A−D type) would thus promote growth in two different orientations, whereas interaction in just one direction (D−A type) would lead to growth in one orientation. The former would form semi-1-D or 2-D nanoribbons, while the latter 1-D nanowires. To further support this proposal, we examined the morphologies of nanostructures obtained from other D−A- and D−A−D-type molecules. Consistent with this proposal, 1-D nanowires and semi-1-D nanoribbons were obtained respectively from other D−A- and D−A−D-type molecules, as shown in Figure 5b and c/d.

However, the nanostructure morphology of the D−A−D-type molecules in Figure 5c and d did not undergo the same change as that of DAPMP; that is, from semi-1-D nanoribbons to 1-D nanotubes/nanowires with increasing temperature, instead the nanostructure remained unchanged as nanoribbons. This behavior is possibly due to the difference in the strength of the dipole−dipole interactions in the two directions. If the difference is large enough, the growth rate in one direction would dominate with increasing processing temperature, and eventually become the predominant growth orientation. Consequently, 1-D nanostructures would only form at higher temperatures. That is to say, the different morphologies are due to different pathways of low-energy molecular stacking at different temperatures.

To clarify further the details of the transformation from 1-D nanotubes to nanowires, we conducted temporal TEM analysis of the formation process of nanotubes at 30 °C.[12] We found

(12) Zhang, X. J.; Zhang, X. H.; Shi, W. S.; Meng, X. M.; Lee, C. S.; Lee, S. T. *Angew. Chem., Int. Ed.* **2007**, *46*, 1525−1528.

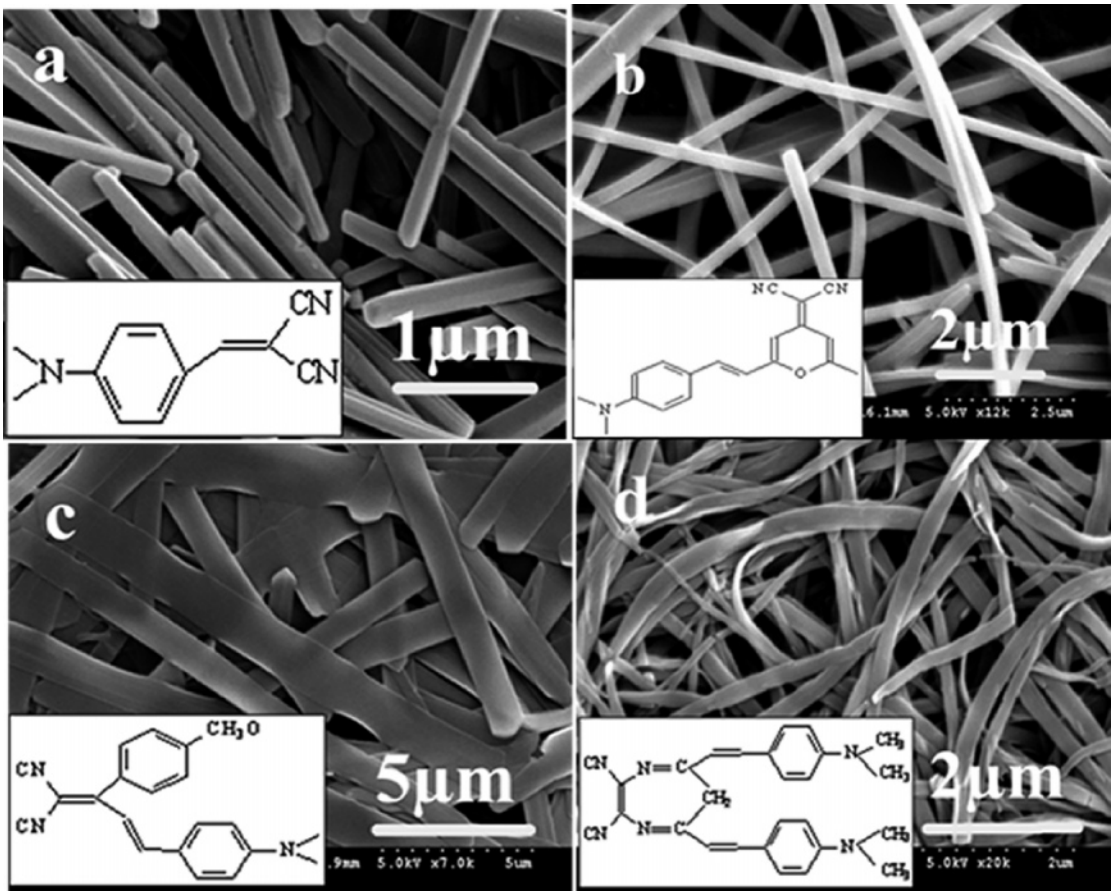

Figure 5. SEM images of nanostructures synthesized from molecules with dipole moment in one direction (a, b) and dipoles in two directions (c, d). Each inset shows the respective molecular structure.

Scheme 1. Energy-Optimized Single Molecule of (a) DAPMP, (b) DPM, and the Possible Aggregation Fashion That Could Form by D−A Dipole−Dipole Intermolecular Interactions

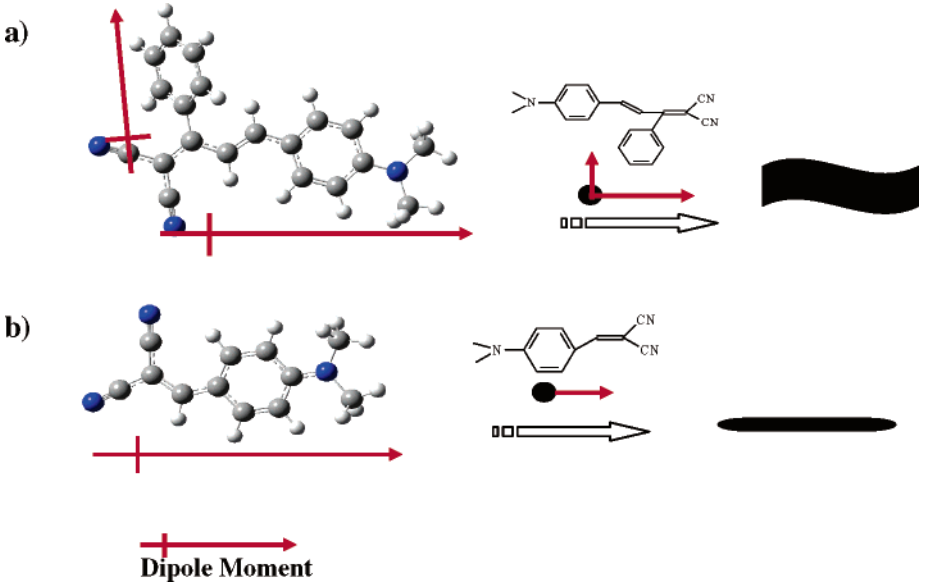

the products obtained right after stirring contained almost all solid nanorods. After 10−20 min, the ends of some nanorods started to curve inward. A high proportion of semitubular nanostructures were formed, and a mixture of nanotubes and nanorods was observed. After about 4 h, almost all of the products transformed into hollow structures (see Supporting Information, Part S2). This phenomenon is similar to the "dissolution" process proposed by Sun et al.[13] for the formation of hematite nanotubes. The process involved coordination-assisted preferential dissolution by phosphate, which started at the tips of the spindle-like nanorods and gradually formed nanotubes by acidic dissolution. In the present system, "dissolution" was caused by the etching effect of THF, which started from the center of the solid rectangular DAPMP nanorods and

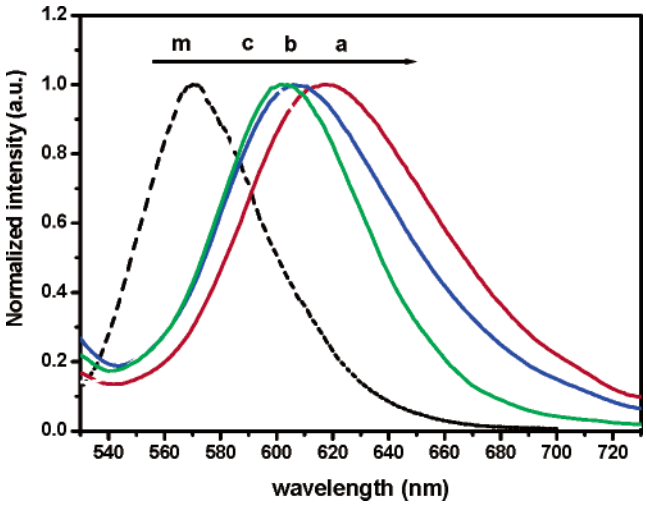

Figure 6. Photoluminescence spectra of DAPMP nanostructures of different morphologies: (a) nanoribbons, (b) nanotubes, and (c) nanowires, while (m) is the spectrum of DAPMP in THF solution (1×10^{-5} mol/L).

continued toward the interior along the long axis[10] to form the nanotubes. As the temperature increased from 30 to 50 and 60 °C under vigorous stirring, some of the THF solvent would evaporate, thus decreasing the etching effect. Therefore, at higher temperature where the etching effect disappears, the products obtained would remain as solid nanorods.

The optical properties of the nanostructures were investigated. The photoluminescence (PL) spectra of the nanostructures demonstrate a distinct morphology-dependent emission, as shown in Figure 6. There is a strong blue shift of the PL peak from 620 to 606 nm as semi-1-D nanoribbons change to 1-D nanotubes, whereas the shift is smaller from 606 to 598 nm as nanotubes change to nanowires. The shift of the PL peak can be attributed to different ways of molecular stacking, and thus different extent of excited-state interaction of DAPMP molecules in the nanoribbons, nanotubes, and nanowires.[7c,14] Nanomaterials with different morphologies also exhibit different optical absorption, which is consistent with the observation that, after sufficient stabilization, the micro-aggregations of nanoribbons and nanotubes would exhibit distinctly different colors of purple and red, respectively (see Supporting Information, Part S3). The differences in the appearance color and PL spectra of different nanostructures of DAPMP support that different stacking fashions are present in different morphological nanostructures, which is also identified by the XRD characterization. Significantly, such morphology-dependent optical properties may provide a novel approach to engineer new optoelectronic devices.

(13) Li, F.; Ding, Y.; Gao, P. X.; Xin, X. Q.; Wang, Z. L. *Angew. Chem., Int. Ed.* **2004**, *43*, 5238−5242.
(14) (a) Allen, N. S. *Polym. Photochem.* **1984**, *5*, 162. (b) Nguyen, T. Q.; Martel, R.; Avouris, P.; Bushey, M. L.; Brus, L.; Nuckolls, C. *J. Am. Chem. Soc.* **2004**, *126*, 5234−5242.

Conclusions

In summary, single-crystal nanostructures of [2-(*p*-dimethyl-aminophenyl)ethenyl]-phenyl-methylene-propanedinitrile (DAPMP) have been prepared by exploiting the strong dipole−dipole interactions between neighboring DAPMP molecules as the driving force. By varying the process temperatures, nanostructures can be readily changed from nanoribbons to nanotubes and to solid nanowires with high morphological purity. Changes in morphology observed are accompanied by changes in optical properties. This unique capability may provide a useful strategy to tune the optical properties of organic nanostructures, which could be exploited as building blocks for nanoscale optoelectronic devices.

Acknowledgment. This work is supported by the Chinese Academy of Sciences, China, CAS-Croucher Joint Laboratory and the National Basic Research Program of China (Grant No. 2006CB933000). S.-T.L. is thankful for support from the NSFC/RGC Joint Research Scheme (N_CityU125/05) of the Research Grants Council of Hong Kong SAR, China. We thank Prof. Wensheng Shi for discussions, Prof. Xiangmin Meng for TEM characterization, and Dr. Jianhua Zhou and Xuyan Xue for computation assistance.

Supporting Information Available: XRD analysis of DAPMP nanoribbons, nanotubes, and nanowires (Part S1), TEM images of DAPMP samples obtained at different times after stirring (Part S2), and the image of nanowires, nanotubes, and nanoribbons (Part S3). This material is available free of charge via the Internet at http://pubs.acs.org.

JA0642109